

Research Article

Yonggui Zhu and Xiaoman Liu

A fast method for L1–L2 modeling for MR image compressive sensing

Abstract: We use a positive parameter to develop a differentiable perturbed reconstruction model to solve the L1–L2 magnetic resonance image (MRI) reconstruction problem. We use Bregman iterative formulation to solve the differentiable perturbed L1–L2 model, and lagged diffusivity fixed-point iteration to solve the minimization problem in the Bregman iteration. Two Fourier transforms and an inverse Fourier transform are used to accelerate L1–L2 MRI reconstruction. Real MR images are used to test the method in numerical experiments. The results demonstrate that the proposed method is very efficient for L1–L2 MRI reconstruction.

Keywords: Compressive sensing, sparse transform, lagged diffusivity fixed-point iteration, Bregman iterative regularization

MSC 2010: 65N21, 49K35, 49K30, 65Q30, 90C47

Yonggui Zhu, Xiaoman Liu: School of Science, Communication University of China, Beijing 100024, P. R. China, e-mail: ygzhu@cuc.edu.cn, xiaoman@cuc.edu.cn

1 Introduction

Compressive sensing (CS) can significantly reduce the scan time in magnetic resonance imaging (MRI) [3, 4]. For CS-MRI, it is possible to accurately reconstruct MR images from undersampled k -space data (i.e., partial Fourier data) by solving nonlinear optimization problems [2]. Suppose $u \in \mathbb{R}^N$ ($N = m \times n$) is a vector formed by stacking the columns of a two-dimensional MR image array $(u_{i,j})$, $i = 1, \dots, m$, $j = 1, \dots, n$, and $u' \in \mathbb{R}^N$ is a sparse or compressive representation for MR image $u \in \mathbb{R}^N$ with respect to basis Ψ , i.e., $u' = \Psi u$. Let $K = \|u'\|_0$ be the number of nonzero elements in u' , and let H denote an $M \times N$ ($M \ll N$) measurement matrix such that $Hu = b$, where b is an observed data vector. Then recovery of u from b is equivalent to solving the L_0 problem

$$\min_u \{\|\Psi u\|_0 : Hu = b\}. \quad (1.1)$$

However, (1.1) is a provably NP-hard problem [11] and very difficult to solve from the viewpoint of numerical computation. Thus, it is realistic to solve the L_1 problem

$$\min_u \{\|\Psi u\|_1 : Hu = b\}, \quad (1.2)$$

which yields sparse solutions under some conditions [5].

In the case of CS-MRI, H is a partial Fourier matrix, i.e., $H = PF$, P is a matrix that consists of $M \ll N$ rows of the identity matrix of size N , and F is an $N \times N$ discrete Fourier matrix. When b is contaminated with noise such as Gaussian noise of variance σ^2 , the relaxation form for problem (1.2) is given by

$$\min_u \{\|\Psi u\|_1 : \|Hu - b\|_2^2 \leq \sigma^2\}. \quad (1.3)$$

The unconstrained version of (1.3) is

$$\min_u \|\Psi u\|_1 + \frac{\mu}{2} \|Hu - b\|_2^2,$$

that is,

$$\min_u \|\Psi u\|_1 + \frac{\mu}{2} \|PFu - b\|_2^2, \quad (1.4)$$

where μ is a positive parameter that determines the trade-off between the fidelity term and the sparsity term, and $\|\cdot\|_2$ denotes the Euclidean norm. Since

$$u' = \Psi u,$$

we have

$$\min_{u'} \|u'\|_1 + \frac{\mu}{2} \|PF\Psi^{-1}u' - b\|_2^2. \quad (1.5)$$

The term

$$\|u'\|_1 = \sum_{i=1}^m \sum_{j=1}^n |u'_{i,j}|$$

is not differentiable; this difficulty can be overcome using the perturbed form

$$\|u'\|_{1,\beta} = \sum_{i=1}^m \sum_{j=1}^n \sqrt{(u'_{i,j})^2 + \beta},$$

where β is a small positive parameter. Therefore, the perturbed form of (1.5) is

$$\min_u \|u'\|_{1,\beta} + \frac{\mu}{2} \|PF\Psi^{-1}u' - b\|_2^2. \quad (1.6)$$

The objective functional in this modified model is differentiable with respect to variable u' . According to the above discussion, we can regard the solution of (1.5) as the limit of the solution of (1.6) when $\beta \rightarrow 0$. Therefore, the solution of (1.6) for small enough β can better approximate the solution of (1.5). To solve (1.6), we can apply version 2 of the Bregman iterative formulation [15]. Bregman iterative regularization for image processing was introduced by Osher, Burger, Goldfarb, Xu and Yin [12]. Assume that

$$J_\beta(u') = \|u'\|_{1,\beta}.$$

According to [15], the Bregman iterative algorithm for solving (1.6) is as follows.

Algorithm 1

$$b^{(0)} \leftarrow 0, u^{(0)} \leftarrow 0$$

for $k = 0, 1, \dots$ **do**

$$b^{(k+1)} \leftarrow b + (b^{(k)} - PF\Psi^{-1}u^{(k)})$$

$$u^{(k+1)} \leftarrow \arg \min_{u'} J_\beta(u') + \frac{\mu}{2} \|PF\Psi^{-1}u' - b^{(k+1)}\|_2^2 \quad (1.7)$$

end for

To solve minimization problem (1.7) in Algorithm 1, we use the lagged diffusivity fixed-point method. The details are discussed in Section 2.

A number of numerical methods have been proposed for solving sparse MRI reconstruction model (1.4). The conjugate gradient (CG) method [9] is a common approach. Other methods include the alternating direction method [14], the operator-splitting algorithm [10], the fast iterative shrinkage-thresholding algorithm [1] and EdgeCS reconstruction [6]. The fast composite splitting algorithm (FCSA) presented by Huang, Zhang and Metaxas in [8] can also be used to solve problem (1.4). Note that FCSA is a state-of-the-art method for CS-MRI reconstruction. Instead of the TV term with nonlocal total variation (NLTV) in FCSA, an NLTV-FCSA algorithm was proposed for MRI reconstruction [7]. In Section 4, we compare our proposed method with the FCSA algorithm.

The remainder of the paper is organized as follows. In Section 2, a fast method for the sparse MR image reconstruction is presented. In Section 3, some real MR images are used to test the effectiveness of our method for sparse MRI reconstruction in numerical experiments. Finally, some concluding remarks are given in Section 4.

Denoting the coefficient matrix associated with the vector $u^{(k+1)}$ on the left-hand side of (2.2) as C , we can obtain

$$Cu^{(k+1)} + \mu\Psi F^* P^* (PF\Psi^{-1}u^{(k+1)} - b^{(k+1)}) = 0. \quad (2.3)$$

That is,

$$Cu^{(k+1)} + \mu\Psi F^* P^* PF\Psi^{-1}u^{(k+1)} = \mu\Psi F^* P^* b^{(k+1)}. \quad (2.4)$$

Multiplying both sides of (2.4) by the operator Ψ^{-1} , we obtain

$$C\Psi^{-1}u^{(k+1)} + \mu F^* P^* PF\Psi^{-1}u^{(k+1)} = \mu F^* P^* b^{(k+1)}. \quad (2.5)$$

Since $u^{(k+1)} = \Psi^{-1}u'^{(k+1)}$, equation (2.5) becomes

$$Cu^{(k+1)} + \mu F^* P^* PFu^{(k+1)} = \mu F^* P^* b^{(k+1)}. \quad (2.6)$$

Multiplying both sides of (2.6) by the Fourier matrix F and using the fact that $FF^* = I$, we obtain

$$CFu^{(k+1)} + \mu P^* PFu^{(k+1)} = \mu P^* b^{(k+1)}. \quad (2.7)$$

Let $D = C + \mu P^* P$. Then D is a diagonal matrix. Therefore, (2.7) becomes

$$DFu^{(k+1)} = \mu P^* b^{(k+1)}. \quad (2.8)$$

Thus, we can quickly obtain $Fu^{(k+1)}$ by (2.8). Then we apply the operator F^* to obtain $u^{(k+1)} = F^*(Fu^{(k+1)})$. Computing $u^{(k+1)}$ involves two fast Fourier transforms (FFTs) and one inverse FFT, so obtaining $u^{(k+1)}$ by the above method is fast. Using this acceleration method to obtain $u^{(k+1)}$ in Bregman iterative Algorithm 1 yields a fast algorithm for solving (1.4). This fast method for sparse CS-MRI reconstruction is given as follows.

Algorithm 2

Step 1 Input $b, P, F, \mu > 0$, and $\beta > 0$.

Step 2 Initialization

$$k = 0, \quad b^{(0)} = \mathbf{0}, \quad u^{(0)} = \mathbf{0}.$$

Step 3 Iterations

When (the stopping criterion is not satisfied)

$$\left\{ \begin{array}{l} u'^{(k)} = \Psi u^{(k)}; \\ b^{(k+1)} = b + (b^{(k)} - PFu^{(k)}); \\ \text{Compute } \mu P^* b^{(k+1)}, \mu P^* P, C \text{ and } D; \\ \text{Compute } Fu^{(k+1)} \text{ by (2.8)}; \\ \text{Compute } u^{(k+1)} \text{ by } F^*(Fu^{(k+1)}); \\ k = k + 1. \end{array} \right.$$

}

Note that the diagonal property of matrix D and the FFT mean that Algorithm 2 is much faster than other iterative reconstruction methods. In Section 3, we describe numerical experiments to show that our method is very efficient for sparse MRI reconstruction.

3 Numerical experiments

In this section, we assess the performance of Algorithm 2 in solving model (1.4) for CS-MRI. We compare our method with FCSA [8], the state-of-the-art method for CS-MRI.

The signal-to-noise ratio (SNR) is used to measure the quality of reconstructed images and the ratio is defined as

$$\text{SNR} = 20 \log_{10} \left(\frac{\|u_o\|_2}{\|u_o - u\|_2} \right), \quad (3.1)$$

where u and u_o are the reconstructed and original images, respectively. CPU time is used to evaluate the speed of MRI reconstruction. All experiments were performed in MATLAB on a laptop with an Intel Core Duo P8400 processor and 2 GB of memory.

In the first test, we assume strong additive Gaussian noise exists with mean 0 and standard deviation of 2,000. We also choose $\mu = 0.001$ and $\beta = 10^{-3}$. The sampling ratio is defined as M/N , where M and N were introduced in Section 1. The stopping criterion is that the relative difference between successive iterates for the reconstructed image should satisfy

$$\frac{\|u^{(k)} - u^{(k-1)}\|_2}{\|u^{(k)}\|_2} < 10^{-3}. \quad (3.2)$$

We used our algorithm for reconstruction of a brain MR image. Figure 1 (a) shows the original 210×210 brain MR image and Figure 1 (b) shows 33 radial lines in the frequency space for the image. If the MR image is sampled with 33 views in the frequency space, its sampling ratio is 16.81%.

The image reconstructed using our method is shown in Figure 2 (a). The SNR is 14.5455 dB and the CPU time is 0.7500 s. The image reconstructed using FCSA is presented in Figure 2 (b). The SNR is 14.3735 dB and the CPU time is 3.8281 s. The results demonstrate that our method requires a shorter CPU time to yield almost the same SNR.

In the next test we use 55 views in the frequency space with sampling ratios of 27.05% for reconstruction using the two methods. Figure 3 shows the reconstruction results for our method and FCSA when the stopping criterion is satisfied. The corresponding SNR and CPU time are 18.5718 dB and 0.7810 s for Algorithm 2 and 17.9143 dB and 3.7593 s for FCSA with 55 views.

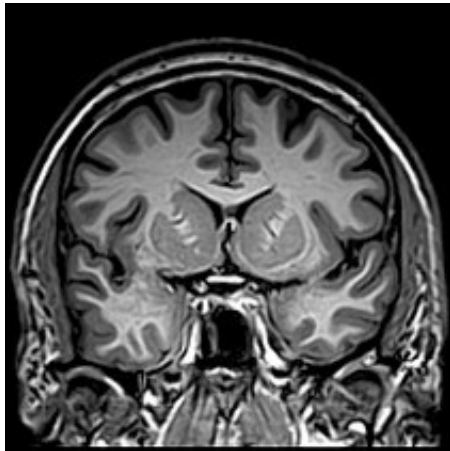
From the CPU time and SNR values for images reconstructed by our method and FCSA, it is evident that our method is five times faster than FCSA while the SNR is greater for our method than for FCSA.

Table 1 lists SNR and CPU time values for our method and FCSA when the stopping criterion is satisfied under different sampling ratios.

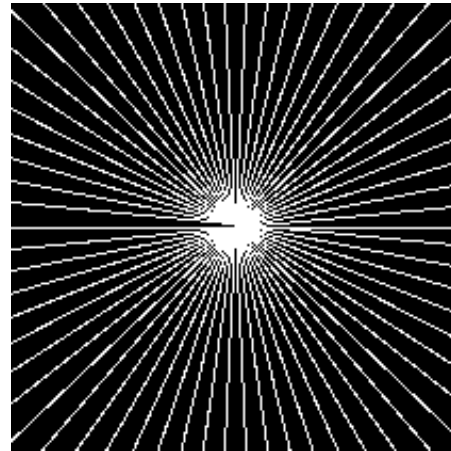
Sampling ratio (views)	Method	SNR (dB)	CPU (s)
16.81% (33)	Our method	14.5455	0.7500
	FCSA	14.3735	3.8281
22.60% (44)	Our method	17.2935	0.7970
	FCSA	16.0484	3.6250
27.05% (55)	Our method	18.5718	0.7810
	FCSA	17.9143	3.7593
32.10% (66)	Our method	18.9542	0.7512
	FCSA	18.0442	3.8906
36.71% (77)	Our method	18.7455	0.7935
	FCSA	17.8494	3.8281
41.54% (88)	Our method	18.3991	0.7832
	FCSA	17.6112	3.8750
45.58% (99)	Our method	18.1329	0.7820
	FCSA	17.3724	3.9219

Table 1. SNR and CPU time data for reconstruction using our method and FCSA.

The results in Table 1 reveal that the SNR is slightly greater for our method than for FCSA. In addition, the CPU time is much less for our method than for FCSA for MRI reconstruction under strong noise.

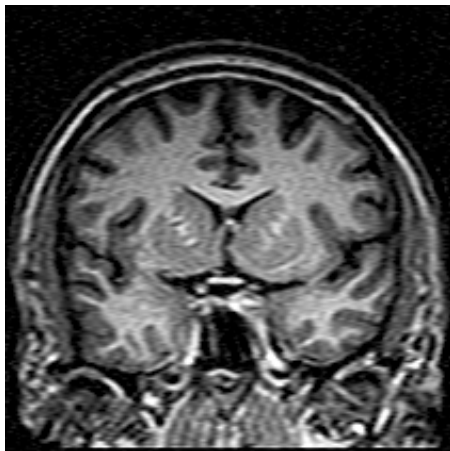


(a) Original image.

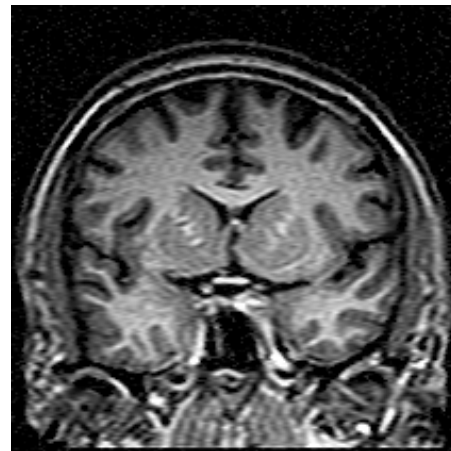


(b) 33 views in the frequency space.

Figure 1

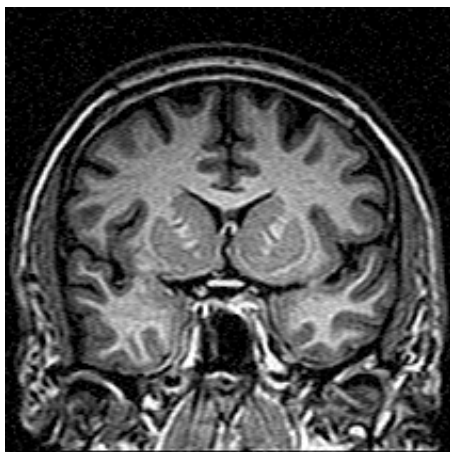


(a) Image reconstructed by our method.

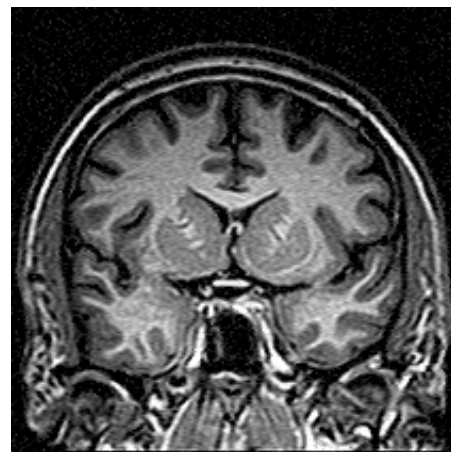


(b) Image reconstructed by FCSA.

Figure 2



(a) Image reconstructed by our method.



(b) Image reconstructed by FCSA.

Figure 3

Figure 4 (a) shows a 924×208 MR body image. This was sampled according to the mask shown in Figure 4 (b), where white pixels indicate sampled locations in k -space. The corresponding sampling ratio is 28.92%. We assumed a mean and standard deviation for additive Gaussian noise of 0 and 2,000, with $\mu = 0.001$ and $\beta = 10^{-3}$. The reconstruction results for our method and FCSA when the stopping criterion is satisfied are shown in Figure 4 (c)–(d). The SNR and CPU time are 17.3696 dB and 3.0780 s for Algorithm 2 and 16.7074 dB and 13.8750 s for FCSA, respectively. Thus, the SNR and CPU time for image reconstruction are better for our method than for FCSA.

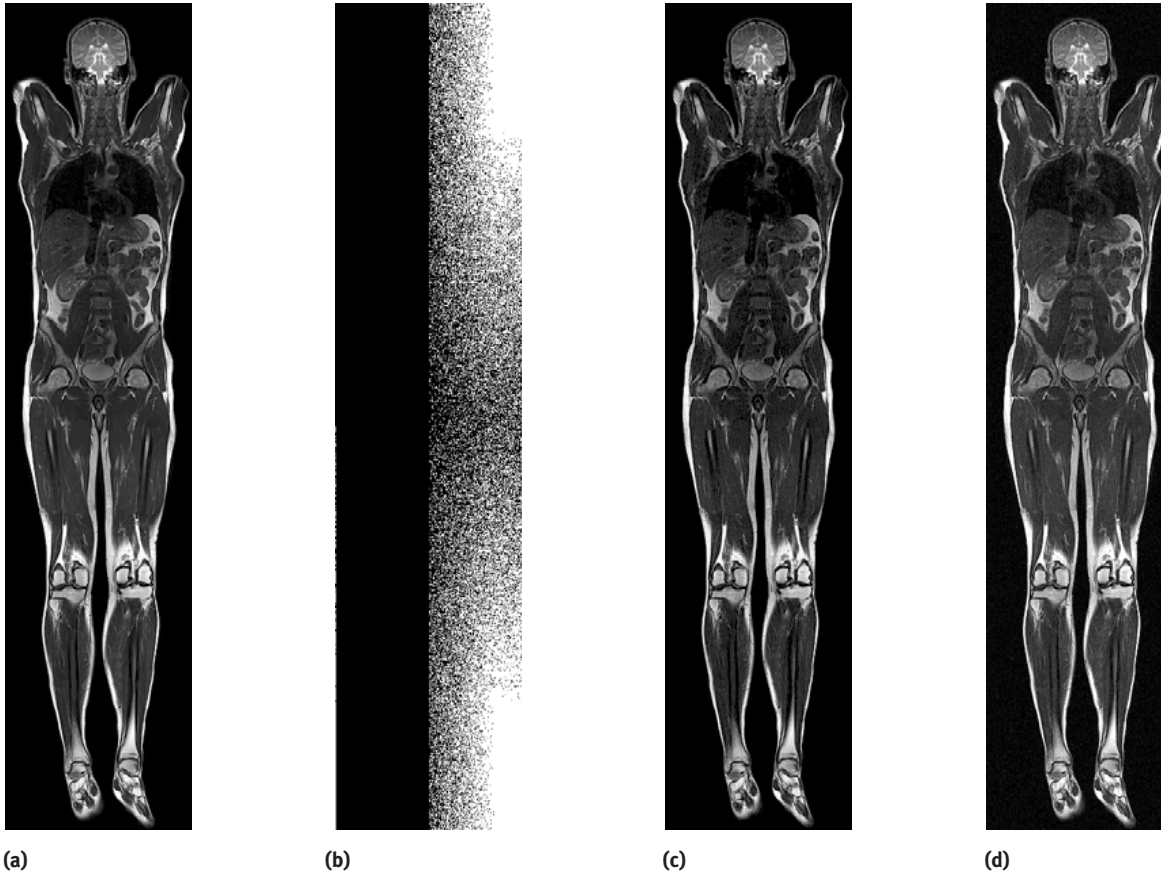


Figure 4. Original image, sampling mask, and images reconstructed using our method and FCSA.

Finally, Figure 5 shows curves for SNR and CPU time for our method and FCSA when the stopping criterion is satisfied under different sampling ratios. The curves show that the SNR is greater for our method than for FCSA. In addition, the CPU time is much less for our method than for FCSA.

4 Conclusion

A sparse L1–L2 MRI reconstruction model was changed to a differentiable perturbed reconstruction model by adding a positive parameter β . Bregman iteration was used to solve the differentiable perturbed L1–L2 reconstruction model. Lagged diffusivity fixed-point iteration was used to solve the minimization problem in the Bregman iteration. Two Fourier transforms and an inverse Fourier transform were used to accelerate sparse L1–L2 MRI reconstruction. The fast method was compared with FCSA, the state-of-the-art method. Real brain MR images were used to test our approach in numerical experiments. The reconstruction results demonstrate that our method for solving model (1.4) is very efficient for sparse MRI reconstruction.

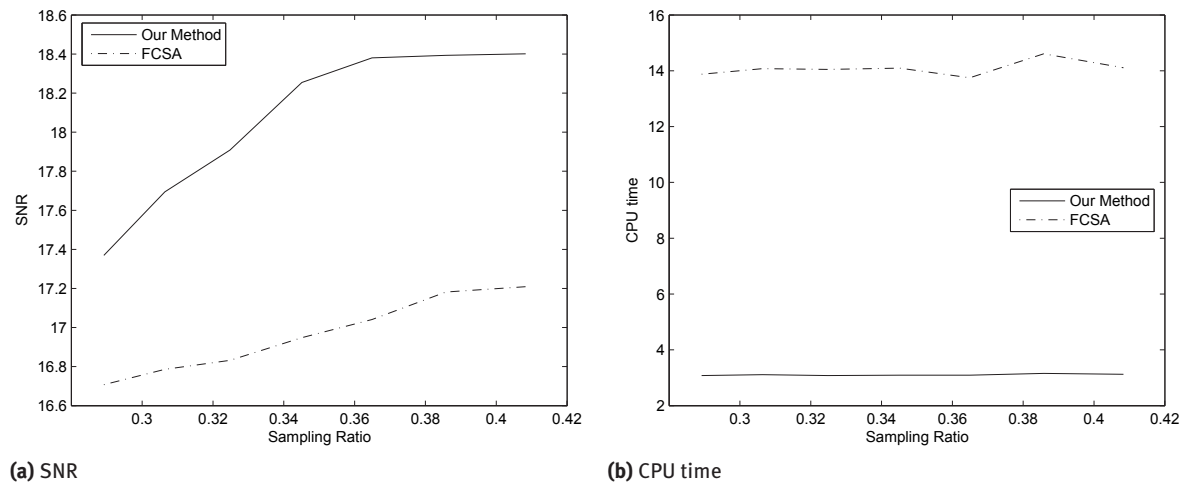


Figure 5. SNR and CPU time for images reconstructed using our method and FCSA for various sampling ratios.

Funding: This work was supported by Key Projects of the Chinese Ministry of Education (No. 109030) and Science Research Projects of CUC (No. XNL1203).

References

- [1] A. Beck and M. Teboulle, A fast iterative shrinkage-thresholding algorithm for linear inverse problems, *SIAM J. Imaging Sci.* **2** (2009), no. 1, 183–202.
- [2] E. J. Candes and J. Romberg, Sparsity and incoherence in compressive sampling, *Inverse Problems* **23** (2007), no. 3, 969–985.
- [3] E. J. Candes, J. Romberg and T. Tao, Robust uncertainty principles: Exact signal reconstruction from highly incomplete frequency information, *IEEE Trans. Inf. Theory* **52** (2006), no. 2, 489–509.
- [4] D. L. Donoho, Compressed sensing, *IEEE Trans. Inform. Theory* **52** (2006), no. 4, 1289–1306.
- [5] J. J. Fuchs, On sparse representations in arbitrary redundant bases, *IEEE Trans. Inform. Theory* **50** (2004), no. 6, 1341–1344.
- [6] W. Guo and W. Yin, Edge guided reconstruction for compressive imaging, *SIAM J. Imaging Sci.* **5** (2012), no. 3, 809–834.
- [7] J. Huang and F. Yang, Compressed magnetic resonance imaging based on wavelet sparsity and nonlocal total variation, in: *IEEE International Symposium on Biomedical Imaging – ISBI’12*, IEEE Press, Piscataway (2012), 968–971.
- [8] J. Huang, S. Zhang and D. Metaxas, Efficient MR image reconstruction for compressed MR imaging, *Medical Image Anal.* **15** (2011), no. 5, 670–679.
- [9] M. Lustig, D. Donoho and D. Pauly, Sparse MRI: the application of compressed sensing for rapid MR imaging, *Magnetic Resonance Med.* **58** (2007), no. 6, 1182–1195.
- [10] S. Ma, W. Yin, Y. Zhang and A. Chakraborty, An efficient algorithm for compressed MR imaging using total variation and wavelets, in: *IEEE Conference on Computer Vision and Pattern Recognition – CVPR 2008*, IEEE Press, Piscataway (2008), 1–8.
- [11] B. K. Natarajan, Sparse approximate solutions to linear systems, *SIAM J. Comput.* **24** (1995), no. 2, 227–234.
- [12] S. Osher, M. Burger, D. Goldfarb, J. Xu and W. Yin, An iterated regularization method for total variation-based image restoration, *Multiscale Model. Simul.* **4** (2005), no. 2, 460–489.
- [13] C. R. Vogel and M. E. Oman, Iterative methods for total variation denoising, *SIAM J. Sci. Comput.* **17** (1996), no. 1, 227–238.
- [14] J. Yang, Y. Zhang and W. Yin, A fast alternating direction method for TVL1-L2 signal reconstruction from partial Fourier data, *IEEE J. Sel. Topics Signal. Process.* **4** (2010), no. 2, 288–297.
- [15] W. Yin, S. Osher, D. Goldfarb and J. Darbon, Bregman iterative algorithms for L1-minimization with applications to compressed sensing, *SIAM J. Imaging Sci.* **1** (2008), no. 1, 143–168.

Received August 14, 2013; revised February 2, 2014; accepted August 15, 2014.